DYNAMIC VALIDATION OF ROLLOVER BUCK ROOF STRUCTURE

Jacek Toczyski
Qi Zhang
Patrick Foltz
Brian Overby
Jim Bolton
Joey White
John Moors
Jack Cochran
Carolyn Roberts
Jeff Crandall
Jason Kerrigan
Center for Applied Biomechanics, University of Virginia
United States

Paper Number 15-0336

ABSTRACT

Effective passive countermeasure design for rollover injury prevention requires thorough understanding of the occupant response in rollover impact. Thus, the dummy biofidelity in rollover crashes is important. To evaluate the dummy biofidelity a test buck was developed for a variety of surrogate biofidelity analyses. The buck was designed to mimic the geometry and inertial properties of a modern strong-roof vehicle. It consisted of two major parts: a deformable, replaceable greenhouse and a rigid base. The goal of this study was to show that the greenhouse structure proposed in this paper, when loaded in a static roof crush test (similar to FMVSS 216) reaches the strength-to-weight ratio level of real vehicles and when loaded in a dynamic rollover test, the roof deformation matches deformation magnitude and shapes observed in the vehicles from the current United States (US) fleet. To achieve this goal a multi-step design approach was used, including a quasi-static roof crush test and a rollover test on fabricated prototypes of the buck roof structure. Based on the gathered data, modifications were introduced to the roof design to improve the greenhouse mechanical response, both dynamically and quasi-statically. Once the design was fixed, one additional static and twelve dynamic rollover tests were performed and roof structure deformation was compared to the measurements made on two late-model US-market vehicles (an SUV and a mini-van), tested in similar conditions. The roof exhibited a desired response under the quasi-static loading with the peak value (61.1 kN) within first 127 mm of platen motion, which resulted in the strength-to-weight ratio of 3.76. During the twelve rollover tests the magnitude and shape of the buck roof deformation were consistent with those measured on the two test vehicles. In the twelve tests the maximum resultant displacements of the trailing side A- and B-pillar (after excluding three outlier tests due to welding defects) were as follows: 189-223 mm and 183-222 mm, respectively. The component displacements of the B-pillar were: between 165-198 mm in SAE Y and between 84-106 mm in SAE Z. The results of this study showed that the designed roof structure can match the deformation magnitude and shapes, including the prevalence of greater lateral than vertical displacement, seen in the current US fleet vehicles. The roof developed in this study has a quasi-static response similar to that of real vehicles loaded in a FMVSS 216-like test. It mimics the stiffness of real vehicle roofs under static and dynamic roof crush loading, and thus it can be used with the test buck to simulate real vehicle rollover crashes to perform parametric analyses and evaluate dummy biofidelity.

INTRODUCTION

Rollover crashes present a challenge to improve occupant safety. Effective passive countermeasure design for rollover injury prevention requires thorough understanding of the occupant response in rollover impact. NHTSA showed in one of its research notes that higher roof strength results in lower roof deformation during a rollover crash (NHTSA 2010). The lower roof deformation was previously correlated to reduction in injury risk to the head, neck, or face (Austin et al. 2005).

Currently in the United States (US), the only Federal Motor Vehicle Safety Standard (FMVSS) used for evaluating vehicle crashworthiness in rollover is FMVSS 216 that assesses the stiffness of the vehicle greenhouse structure in a quasi-static roof crush test. While numerous dynamic test methods (e.g. ramp test, curb-trip rollover test, dolly test, etc.) were developed and used to evaluate rollover crash dynamics, vehicle crashworthiness, and occupant injury risk, these methods were criticized for their lack of repeatability. To investigate the crash test dummy biofidelity in rollover-like scenarios, the University of Virginia Center for Applied Biomechanics is planning to compare crash dummy response to post-mortem human surrogate (PMHS) response in a series of experimental rollover investigations. To perform these tests, a vehicle-like test buck was developed. The buck was designed to mimic the geometric and inertial properties of twelve late-model full-size crossover vehicles or mid-size sport utility vehicles (SUV) from the US fleet, including BMW X5, Ford Explorer, Volkswagen Touareg and Volvo XC90. The buck is to be used in the biofidelity tests for a variety of reasons. Primarily, with the use of the test buck exact tests without relying upon a particular vehicle design can be repeated, even after several years from now. Secondly, the simplified buck allows for utilizing 3-d optical motion capture systems that have been used to characterize occupant surrogate motion in simulated crash tests (cf. Lessley et al. 2010). Using such a system provides detailed 3-d kinematics data that can be used to make intricate comparisons between crash test dummies and PMHS.

To evaluate dummy biofidelity during the injury causing parts of the rollover crash, a buck roof structure that matches modern vehicle deformations seen in real-world rollover accidents would be beneficial. Hence, the goal of this study was to show that the greenhouse structure described in this paper, when loaded in a static roof crush test (similar to FMVSS 216) meets the strength-to-weight ratio (SWR) level of cars with strong roofs and when loaded in a dynamic rollover test, the roof deformation matches deformation magnitude and shapes, including the prevalence of greater lateral than vertical displacement, observed in late-model US-market vehicles.

STEP 1 – 1st ROOF DESIGN FABRICATION

The current study is a continuation of the study presented by Toczyski et al. in 2013. The previous study was carried out using finite element (FE) analyses to facilitate computationally and monetarily inexpensive evaluations of iterative changes to the roof structure design. Each of the roof component sections were sized by performing a detailed computational investigation using a commercial implicit FE code. A multi-tiered design approach was used, consisting of different – in terms of complexity – FE models of the roof, to better understand the quasi-static response of the structure in a 216-like roof crush test. Variations in an initial design of the greenhouse and computational analyses yielded a model that had a loading response representative of a modern full-size crossover vehicle. Based on that work the design of the roof was fixed. It was accomplished by modeling off-the-shelf parts in a way that made the roof easily fabricated. The next step was to manufacture the roof and examine its response in real tests (both, statically and dynamically).

STEP 2 – 1ST QUASI-STATIC ROOF CRUSH TEST

The fabricated greenhouse structure was tested first in a static roof crush test similar to the roof resistance test described in the FMVSS No. 216 (NHTSA 2012). The roof was attached to the parametric buck rigid base (cf. Zhang et al. 2013). The structure was then loaded at a 25 degree roll and a 5 degree pitch angle, with a rigid platen. The platen was driven into the buck for a distance of 254 mm, and the peak reaction force on the platen generated in the first 127 mm of deformation was normalized by the test buck weight to determine the strength-to-weight ratio. SWR was calculated using two different buck masses: (1) the mass including the base and the greenhouse structure, all the instrumentation, high speed camera equipment, weight ballast, etc. needed to run a rollover test, but without occupants; (2) the mass with all needed equipment and one 80 kg occupant. The mass was found to be 1657 kg and 1737 kg, respectively. After the test all components and connections which fractured within the first 127 mm of platen motion were documented.

In the roof design the connections between the pillars, roof rails and the buck base utilized plastic joints, consisting of a round bar set into the tube ends (Figure 1a). One straight round bar was used to connect the AB to the BC roof rail. The round bar coming out of the B-pillar was then welded to the bar connecting the rails creating a "T-like" shape (Figure 1a). The C-pillars and the BC and CD rails were linked in the same way. During the first quasi-static roof test the four welds between the pillars and the rails fractured. The first weld broke after 48 mm of

platen displacement. After that point the load-bearing capabilities of the greenhouse structure were significantly reduced, which resulted in a peak force of 23.3 kN within first 127 mm of platen motion (Figure 1b; blue dotted curve) and SWR equaled to 1.43 (without including the occupant's weight in the overall buck weight) and 1.37 after including an 80 kg occupant. Based on the test data it was determined that the friction coefficient between the roof structure and the platen was between 0.2 and 0.3.

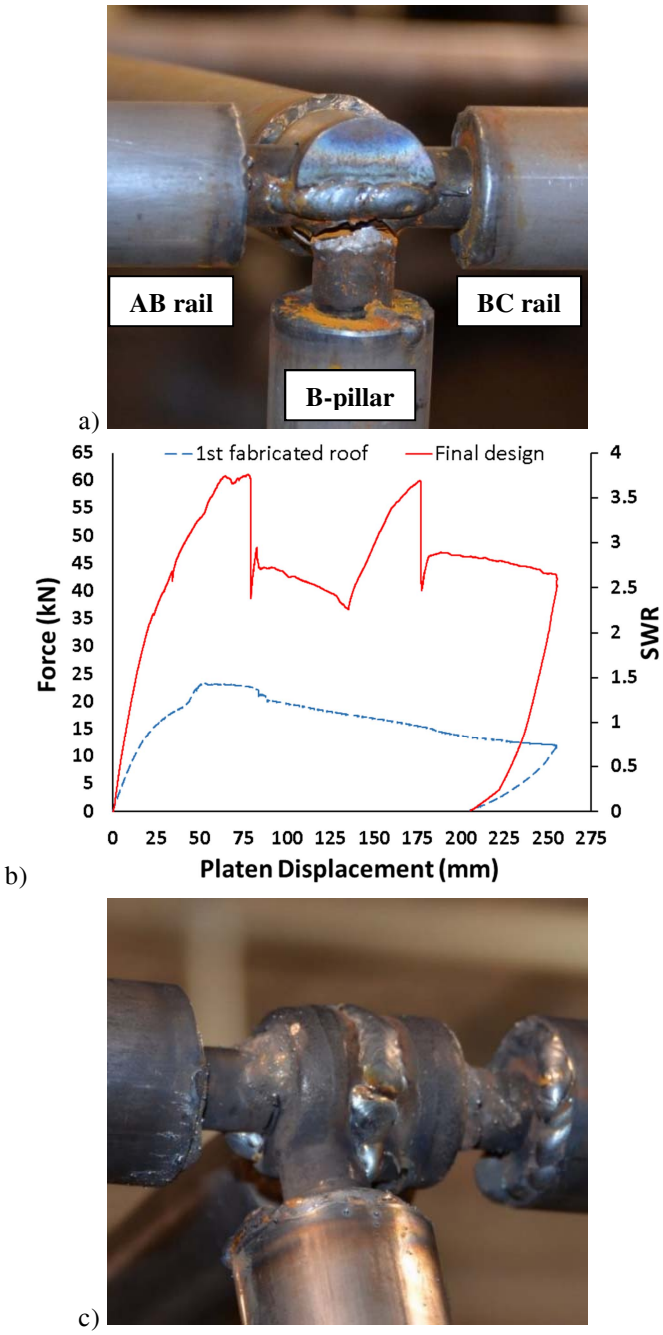

Figure1. a) Fracture of one of the "T-like" top joints; b) 216 test-like results for the 1st and the final design of the roof structure; c) one of the modified top joints (eye bot used).

In the next design the connections between the pillars and the roof rails were modified. Instead of a bar coming out of the pillar an eye bolt was used (Figure 1c). A straight bar coming out of the roof rail went through an

eye bolt and was welded to it on both sides around the bar circumference. This created much stronger connections between the components and let the load be distributed more equally in the greenhouse structure. To stiffen up the structure and to simplify the manufacturing process of further roofs it was also decided to uniform the diameter of plastic joints at the interface between the roof and the rigid base (all of them were set to 19 mm) as well as all of the top joints (set to 16 mm). Additionally, a cross bracing (steel bar of diameter of 5.6 mm, working in tension, Figure 3e) between A-, C- and D-pillars was added to increase the structure energy dissipation compatibility under quasi-static loading.

STEP 3 – 1ST ROLLOVER TEST

After the quasi-static test the roof design was modified, the new greenhouse was fabricated, attached to the buck base and then subjected to a passenger-side leading rollover test, with the use of the Dynamic Rollover Test System (DRoTS) fixture (Kerrigan et al. 2011).

To minimize any potential risk of equipment damage during the test, minimal instrumentation was installed on the buck. To ensure the repeatability of the buck response from test to test, ballast was added onto the buck base to account for additional test instrumentation (data acquisition system, cameras, lights, imaging system components, etc.) that might be used in future tests. Two water dummies were also positioned in the driver and passenger seat, respectively. In addition, the buck was instrumented with nine string potentiometers (model 62-60, Firstmark Controls, Creedmoor, NC) to capture and resolve time histories of single point greenhouse deformations into local coordinate system components (cf. Lockerby et al. 2013). Local axes were defined using the Society of Automotive Engineers standard for vehicles (SAE 1995). The cables from three of the potentiometers were joined together and attached to hooks that were welded on the pillars. The time histories were captured for the top of the driver A- and B-pillars, as well as for the passenger B-pillar.

Touchdown conditions for the first rollover buck roof test

To evaluate dummy biofidelity during the rollover crash, a buck roof structure matching modern vehicle deformations (in terms of the magnitude and the shape) seen in real-world rollover accidents was needed. To access the buck roof response in such an event deformation data gathered on real vehicles loaded dynamically in rollover-like scenarios was necessary as a reference point. For the purpose of this study, using the DRoTS fixture, two late-model US-market vehicles (a mid-size SUV and a mini-van) were tested in controlled rollover impact with slightly different test parameters (see Table 1). The vehicles were instrumented either with string potentiometers or an optical measurement system to capture and resolve time histories of single point greenhouse deformations into local vehicle coordinate system components. The touchdown conditions for both of the vehicles were obtained from crash reconstructions of actual crashes:

1) for the SUV they were the result of a reconstruction of a CIREN rollover case (Case 781125527) with an ADAMS multi-body model of the same mid-size SUV (cf. Kim et al. 2014),
2) for the mini-van they were the result of a crash reconstruction of National Automotive Sampling System Crashworthiness Data System (NASS-CDS) case number 2008-03-108.

Both vehicle tests simulated a driver-side leading rollover crash. However, to be consistent with the previous rollover buck kinematic tests (Zhang et al. 2014, Lessley et al. 2014), the rollover buck roof test was intended to simulate a passenger-side leading roll. Because the SUV happened to be one of the late-model full-size crossover or mid-size sport utility vehicles that were used for designing the rollover parametric buck base, for the first buck roof rollover test the SUV touchdown conditions were selected as the test parameters. Therefore, the roll angle and roll rate direction were changed accordingly to be 248 deg/s at a leading-side touchdown at 155 degree roll angle. The vertical velocity 1.1 m/s remained the same as in the vehicle test. In addition, the vehicle touchdown pitch angle was changed to -1.5 degree (pitched forward) to focus more on the A-B pillar responses of the buck roof.

Table1.
Summary of the touchdown conditions for vehicle tests and the rollover buck test goals.

Vehicle	Mid-size SUV	Mini-Van	1st Buck Roof Test	Other Buck Roof Tests (Goals)
Pitch Angle (deg)*	1.4	-7.7	-1.5	-1.5
Roll Angle (deg)**	-155.3	-143.2	155	145
Roll Rate (deg/s)**	-248.2	-245	248	248
Vertical Velocity (m/s)	1.1	1.67	1.1	1.1

* Negative means pitched forward
** Negative means driver-side leading roll

Results from the first rollover buck roof test

The roof deformation data measured by the string potentiometers were processed and presented in the buck local coordinate system (cf. Lockerby et al. 2013). The driver A-pillar recorded peak deformation of 291 mm in Y direction, 237 mm in Z direction and 376 mm resultant deformation. The driver B-pillar recorded peak deformation of 277 mm in Y direction, 184 mm in Z direction and 329 mm resultant deformation. Based on the tested vehicles the maximum deformation goals for the trailing side B-pillar for Y and Z directions were set to be: 166 mm and 94 mm, respectively (Figure 4). In the first buck rollover test the recorded trailing (driver) B-pillar peak deformation in Y direction was approx. 67% higher than the displacement goal and approx. 96% higher than the goal in Z direction.

During the test several components of the structure were broken. The top end (eye bolt) of the passenger B-pillar as well as the driver C-pillar fractured (sheared) at the intersection with the pillar tube (Figure 2a). On both sides of the buck the top of the stands in the B-pillar area were also fractured. The tubes broke close to the welds. In case of the bars, the welds were broken (Figure 2b). To prevent these fractures from happening again several changes were introduced to the structure before fixing the final design:

- material used for the rod ends (eye bolts) was changed from low carbon steel (more brittle) to stainless steel (more ductile),
- without affecting the overall geometry of the roof, the pillar tubes were shortened from the top (for B-, C- and D-pillars) to give the joints more room for bending,
- the top shelves for the B-pillar bar stands were drilled and the bars were put through the shelves to unload the welds and give the stands more support in bending,
- the diameter of the bottom joints of the B- and C-pillars was increased from 19 mm to 22 mm to stiffen up the overall greenhouse response in bending.

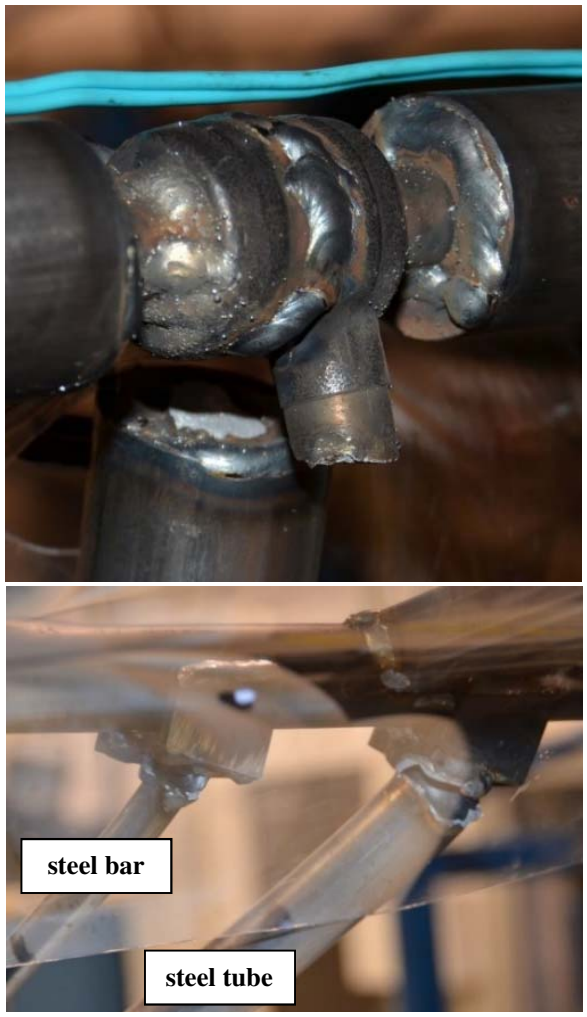

Figure2. Joint fracture: a) passenger B-pillar, b) top connections of the B-pillar stands.

After the test, it was determined that the leading-side roof either missed the roadbed or just barely touched it resulting in no sensor response from the roadbed load cells. This problem was partially caused by the fact that the target touchdown angle (155 degrees) was difficult to achieve. Even a small variation in the relative timing between the vehicle roll angle and vertical travel distance could result in a large variation in the touchdown conditions, or even totally missed the leading-side roof touchdown, making these touchdown conditions difficult to be repeatable from test to test. Hence, it was decided to change – in future tests – the touchdown roll angle to 145 degrees to ensure a more repeatable response of both, the buck and the occupants. To be consistent with the vehicle tests, the new touchdown roll angle was set based on the mini-van test (see Table 1).

STEP 5 – FINAL DESIGN OF THE GREENHOUSE STRUCTURE

Quasi-static roof crush test

Once the roof design was fixed (Figure 3), its structure was again subjected to a 216-like roof crush resistance test. The force-displacement response of the new design can be divided into several phases (Figure 1b, red solid curve). During the first phase (0-65 mm) the platen pushed the A-pillar, the head rail and the AB-roof rail inwards, engaging most of the plastic joints as well as putting the cross bracing between the bottom of the driver-side A-pillar and the top of the passenger-side A-pillar in uniaxial tension. During that phase the force increased monotonically and then – after 65 mm of platen displacement – plateaued around 60 kN. The force reached its maximum value

(61.1 kN) at 78 mm of platen motion. Just after 78 mm the A-pillar cross bracing fractured causing a drop in the force by approx. 30%. In the following phase the force started decreasing nonlinearly until 135 mm of deformation when the C-pillar was engaged. By engaging the pillar the cross bracing between the C-pillars was also engaged, what resulted in a large increase in global roof stiffness. The second peak of the force (60 kN at 177 mm) was observed just before the fracture of the C-pillar bracing. After the bracing breakage the force dropped to approx. 46 kN and started decreasing slightly till the end of the test, when it reached 40 kN. For the maximum force of 61.1 kN recorded on the platen within first 127 mm of its movement the calculated SWR equaled to 3.76 (without including the occupant's weight in the overall buck weight) and 3.59 after including an 80 kg occupant. By implementation of all the changes suggested after the first quasi-static and rollover tests, the SWR increased by approx. 160%.

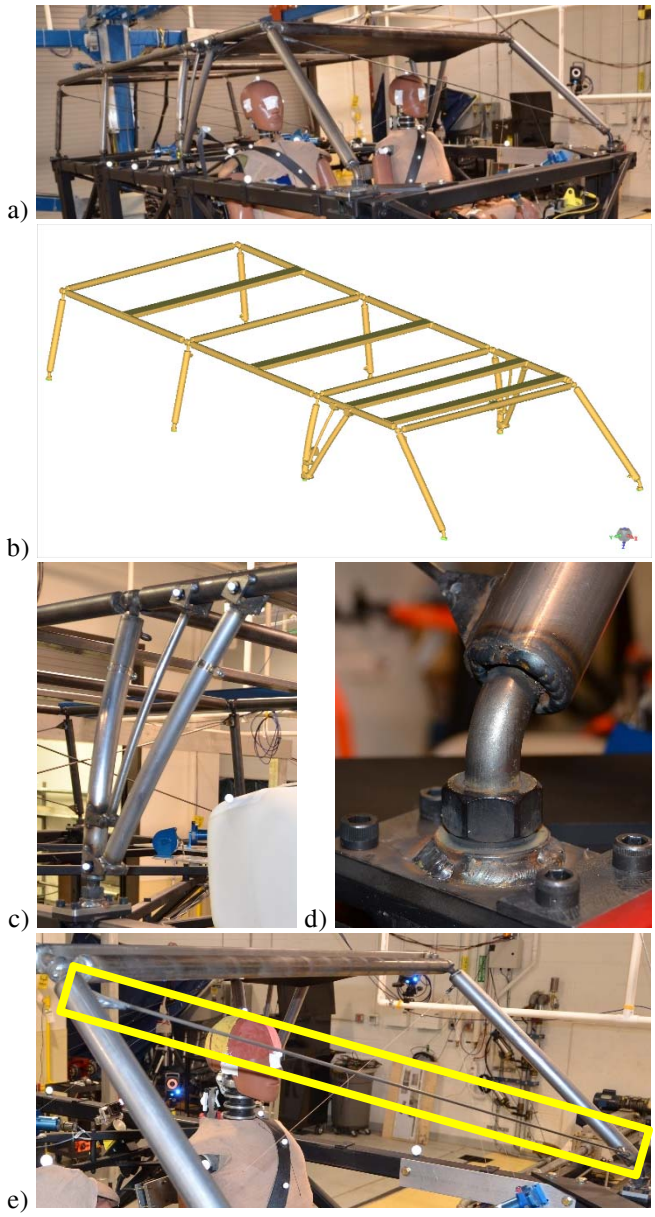

Figure3. The final design of the roof structure: a) isometric view, b) pre-test scan of roof structure (cross bracing between A-, C- and D-pillars not shown), c) steel stands in B-pillar area, d) plastic joint, e) cross bracing between A-pillars.

Twelve rollover tests

With the fixed roof design twelve passenger-side leading rollovers were performed. The actual touchdown parameters achieved in the tests did not varied much and were very close to the goal parameters presented in Table 1, in the "Other Buck Roof Tests" column. The average touchdown angle was 143.4 deg (standard deviation: 1.34 deg; median: 143.4 deg), the average roll rate was 244.6 deg/s (standard deviation: 3.86 deg/s; median: 244.7 deg/s) and the average buck vertical velocity was 1.14 m/s (standard deviation: 0.09 m/s; median: 1.13 m/s).

During the tests the buck was equipped with nine string potentiometers attached to the same points as in the first rollover test. The roof deformation data measured by the string potentiometers were processed and presented (for the driver-side B-pillar; Figure 4) in the buck local coordinate system. After the leading-side touchdown the whole roof structure moved slightly in the negative Y direction and after the trailing-side impact the driver-side pillars and roof rails moved inboard (positive SAE Y) and downward (positive SAE Z). When the roof-to-roadbed interaction ended approx. 0.15 sec after the trailing-side touchdown, elastic unloading of the greenhouse structure occurred.

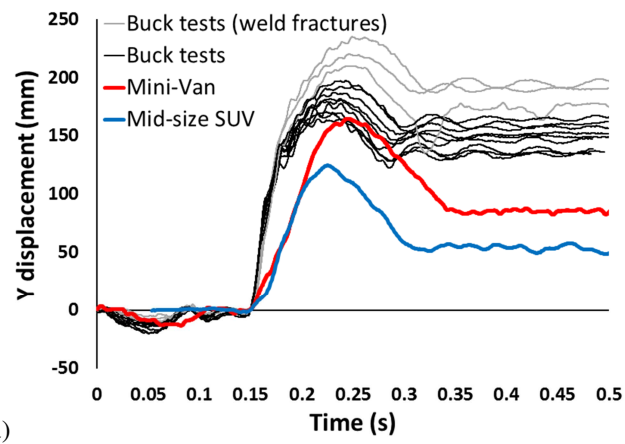

a)

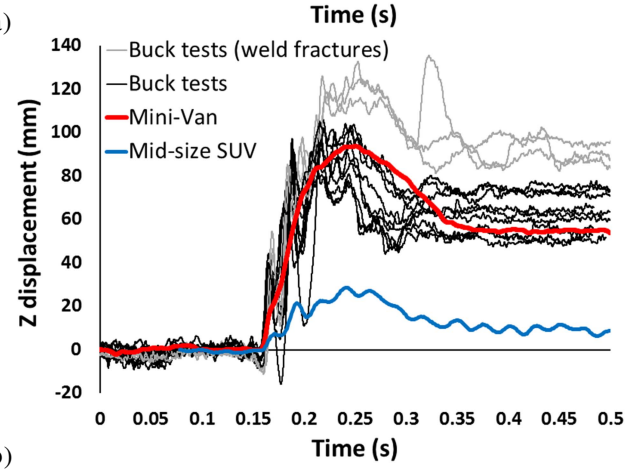

b)

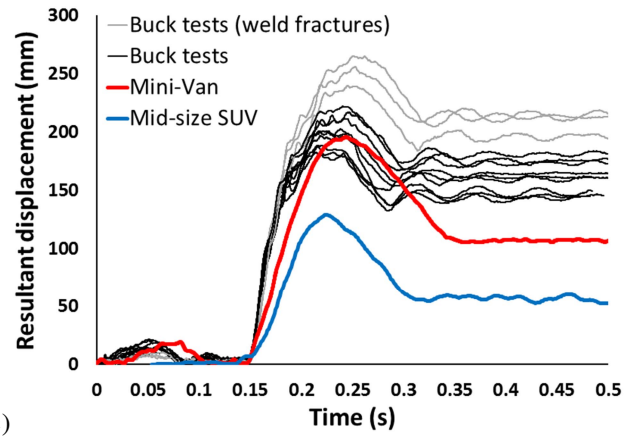

c)

Figure4. Driver B-pillar deformation versus the two test vehicles: a) Y displacement, b) Z displacement, c) resultant displacement.

The driver A-pillar recorded average peak deformation of 205 mm in Y direction (standard deviation: 26 mm; median: 197 mm), 101 mm in Z direction (standard deviation: 15 mm; median: 100 mm) and 229 mm resultant deformation (standard deviation: 30 mm; median: 221 mm). The driver B-pillar recorded average peak deformation of 191 mm in Y direction (standard deviation: 22 mm; median: 185 mm), 103 mm in Z direction (standard deviation: 15 mm; median: 103 mm) and 214 mm resultant deformation (standard deviation: 27 mm; median: 207 mm). It was found that in three out of twelve tests the roof deformation was noticeable larger than in the remaining nine tests. These three tests were marked in gray in Figure 4. After analyzing the post-deformation structure it was determined that in the three tests several connections (mostly at the interface between the roof and the base but also for the stands in the B-pillar area; Figure 5) broke due to welding defects – i.e. the weld did not penetrate the material enough to ensure a proper bond. After excluding these tests from the average deformation calculations the results for the driver A-pillar were as follows: average peak deformation of 188 mm in Y direction (standard deviation: 11 mm; median: 194 mm), 92 mm in Z direction (standard deviation: 10 mm; median: 95 mm) and 209 mm resultant deformation (standard deviation: 14 mm; median: 216 mm). The driver B-pillar average peak deformation was: 180 mm in Y direction (standard deviation: 11 mm; median: 182 mm), 96 mm in Z direction (standard deviation: 9 mm; median: 95 mm) and 201 mm resultant deformation (standard deviation: 14 mm; median: 201 mm). It should be stated here that in all of the performed tests the maximum X displacement component of roof deformation (for all measurement points) varied between ±20 mm from test to test.

a)

b)

Figure5. Weld fractures: a) bottom joint of Driver B-pillar, b) top joint of one of the B-pillar stands.

Before and after one of the twelve rollover tests the greenhouse structure was scanned using a portable measuring arm equipped with a 3D laser scanner (ROMER Absolute Arm Scanner 7330Sl-2, Hexagon Metrology, North Kingstown, RI). After processing the scans, they were aligned together for post-test deformation comparison. It can be observed from the scans that the lateral deformation of the roof was larger than its vertical displacement (Figure 6). Additionally, it can be seen in Figure 6b, that the post deformation in the SAE X direction was much smaller (almost negligible) in comparison with the two other deformation components.

a)

b) 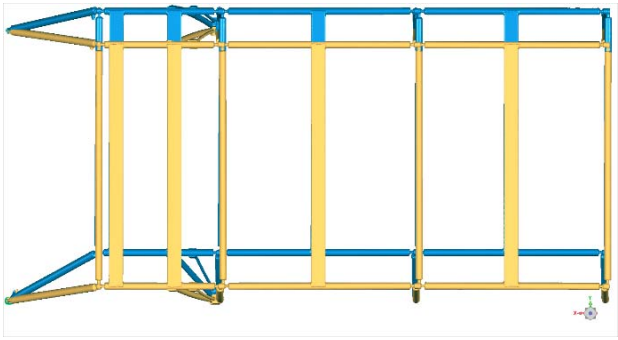

c) 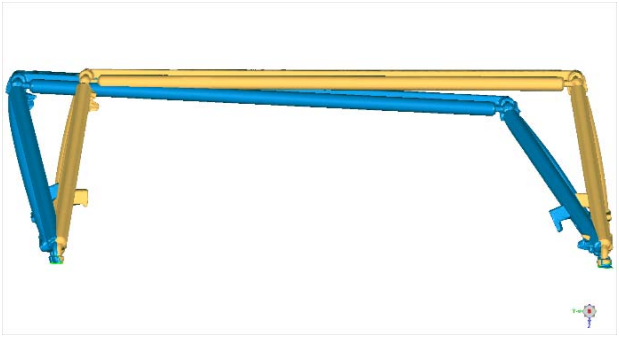

Figure6. Roof deformation for one of the tests (yellow: undeformed; blue: deformed): a) 3D scan isometric view, b) 3D scan top view, c) 3D scan front view.

The roof deformation time histories from the rollover buck tests (for the final roof design) were compared with the vehicle tests at the trailing side B-pillar (Figure 4). It should be noted here that the buck roof tests simulated a passenger-side leading roll crash, while the vehicle tests simulated a driver-side leading roll crash. Therefore the trailing-side B-pillar deformed in the negative Y direction (SAE vehicle local coordinate system) in the vehicle tests, while the trailing-side B-pillar in the buck roof tests deformed in the positive Y direction. The sign of the Y component of the vehicles B-pillar deformation time histories was flipped to facilitate the comparison. In general, the deformation time histories among the buck tests were either in-between or higher than for the tested vehicles. The buck roof structure had less elastic unloading than the vehicles in general. For all the displacement components the roof structure deformation was much closer to the deformation seen in the mini-van test, although in this test the vehicle vertical velocity and the vehicle mass were higher than in the UVA buck roof tests. A direct comparison between the buck roof response and the SUV response created a challenge due to the fact that at touchdown the SUV was pitched backward and the test buck forward. Based on the comparison of the buck results with the two tested vehicles it can be stated that the greenhouse response was softer than the response of the roof structure in the SUV or the mini-van, but still on the same order of magnitude. It can be also seen that the test roof structure matched deformation shapes, including the prevalence of greater lateral than vertical displacement, observed in modern strong-roof cars.

CONCLUSIONS

The roof developed in this study has a quasi-static response similar to that of real vehicles loaded in a FMVSS 216-like test. It mimics the stiffness of real vehicle roofs also under dynamic roof crush loading. The tested roof structure can match the magnitude and shapes of deformation modes seen in the current US fleet vehicles and thus it can be used with the test buck to simulate real vehicle rollover crashes to perform parametric analyses and evaluate dummy biofidelity.

ACKNOWLEDGMENTS

This study was partially supported by the National Highway Traffic Safety Administration (NHTSA) under Cooperative Agreement No. DTNH22-09-H-00247. Views or opinions expressed or implied are those of the authors and are not necessarily representative of the views or opinions of the NHTSA.

REFERENCES

[1] Austin, R., Hicks, M. and Summers, S. 2005. “The Role of Post-Crash Headroom in Predicting Roof Contact Injuries to the Head, Neck, or Face during FMVSS No. 216 Rollovers.” Docket nos. NHTSA-2005-22143 and NHTSA-2005-22154, August 30. Washington, DC: National Highway Traffic Safety Administration.

[2] Kerrigan, J., Jordan, A., Parent, D., Zhang, Q., Funk, J., Dennis, N., Overby, B., Bolton, J. and Crandall, J. 2011. "Design of a dynamic rollover test system." Society of Automotive Engineers (SAE). Paper Number 2011-01-1116. Warrendale, PA
[3] Kim, T., Kerrigan, J., Bollapragada, V., Crandall, J. et al., "Rollover Initiation Simulations for Designing Rollover Initiation Test System (RITS)." SAE Technical Paper 2014-01-0530, 2014, doi: 10.4271/2014-01-0530.
[4] Lessley, D., Shaw, G., Parent, D., Arregui-Dalmases, C., Kindig, M., Riley, P., Purtsezov, S., Sochor, M., Gochenour, T., Bolton, J., Subit, D., Crandall, J.R., Takayama, S., Ono, K., Kamiji, K. and Yasuki, T. 2010. "Whole-body response to pure lateral impact." Stapp Car Crash Journal, Vol. 54, pp. 289-336
[5] Lessley, D., Riley, P., Zhang, Q., Foltz, P., Overby, B., Heltzel, S., Sochor, M., Crandall, J. and Kerrigan, J. 2014. "Occupant Kinematics in Laboratory Rollover Tests: PMHS Response." Stapp Car Crash Journal, Vol. 58, pp. 251-316
[6] Lockerby, J., Kerrigan, J., Seppi, J. and Crandall, J. 2013. "Optical Measurement of High-Rate Dynamic Vehicle Roof Deformation during Rollover," SAE Technical Paper 2013-01-0470, 2013, doi:10.4271/2013-01-0470.
[7] National Highway Traffic Safety Administration (NHTSA). 2010. "Trafic Safety Facts - Roof Strength Testing and Real-World Roof Intrusion in Rollovers." DOT HS 811 365. http://www-nrd.nhtsa.dot.gov/Pubs/811365.pdf
[8] National Highway Traffic Safety Administration (NHTSA). 2012. "Federal Motor Vehicle Safety Standards and Regulations." DOT HS 808 878. http://www.nhtsa.gov/cars/rules/import/fmvss/index.html
[9] Society of Automotive Engineers (SAE). 1995. "Instrumentation for Impact Tests. SAE J211/1 MAR95"
[10] Toczyski, J., Kerrigan, J., Mohan, P. and Crandall, J. 2013. "Design of a deformable vehicle roof structure for rollover crash testing with a test buck." Paper 13-0203, 23rd International Conference on the Enhanced Safety of Vehicles (ESV), Seoul, Korea
[11] Zhang, Q., Kerrigan, J., Lessley, D., Seppi, J., Riley, P., Foltz, P., Lockerby, J., Overby, B., Sowers, C. and Crandall, J. 2013. "Whole-body Kinematics: Response Comparison of the Hybrid III and Hybrid III Pedestrian ATD in DRoTS Rollover Tests." Paper IRC-13-40. 2013 IRCOBI Conference Proceedings, Gothenburg, Sweden
[12] Zhang, Q., Lessley, D., Riley, P., Toczyski, J., Lockerby, J., Foltz, P., Overby, B., Seppi, J., Crandall, J. and Kerrigan, J. 2014. "Occupant Kinematics in Laboratory Rollover Tests: ATD Response and Biofidelity." Stapp Car Crash Journal, Vol. 58, pp. 317-360